REASSESSMENT OF 26AL/27AL RATIOS AMONG CHONDRULES IN Y-81020 (CO3.05). N. T. Kita[1], A. T. Hertwig[1,2], P. E. Sobol[1], M. J. Spicuzza[1], [1]WiscSIMS, Department of Geoscience, University of Wisconsin-Madison, Madison, WI 53706 (kita@wisc.edu), [2]Department of Earth, Planetary, and Space Sciences, UCLA, CA 90095.

Introduction: The chronology of chondrules using ^{26}Al-^{26}Mg system (half-life: 0.705 Ma) provides time resolution for their relative formation ages as short as 0.1 Ma [1]. The total range of chondrule ages within a single chondrite group is expected to be short if they formed under high dust density where planetesimal accretion could occur [2-3]. A short timescale of chondrule formation (i.e. 0.2 Ma) would prevent mixing of materials from large heliocentric distances. In contrast, chondrules from 2 AU and 4 AU would be fully mixed, if they did not accrete to asteroids for > 1 Ma [4], due to radial transport in the protoplanetary disk.

The inferred initial $(^{26}Al/^{27}Al)_0$ ratios of chondrules in Y-81020 (CO3.05) span a wide range from ~1×10^{-5} to ~2×10^{-6} [5-6], or from 1.7 Ma to ~3 Ma after CAI formation (using the canonical ratios of 5.25×10^{-5} from CV CAIs [7]). The ^{26}Al ages from FeO-rich (type II, oxidized) chondrules tend to be younger than those of FeO-poor (type I, reduced) chondrules. Type II chondrules contain Na-rich plagioclase, in which Mg self-diffusion is very fast [8]. Therefore, even for the Y-81020 with low subtypes (3.05), we may not be able to preclude a possible disturbance of the Al-Mg system in the type II chondrules. Here, we re-examine Al-Mg isotope system of four chondrules from [6] by applying the improved SIMS analytical protocols.

Samples: Four chondrules in Y-81020 (NIPR section 56-1) were selected for the SIMS Al-Mg isotope analyses. Chondrule Y23 is an Al-rich chondrule (ARC), which consists of anorthite and high Ca pyroxene. Chondrules Y46, Y56, and Y58 are type II chondrules, which contain plagioclase with intermediate compositions (An_{40-60}). Plagioclase crystals in these chondrules are small (≤10 μm). The $(^{26}Al/^{27}Al)_0$ of Y23, Y46, Y56, and Y58 reported by [6] were $(4.1\pm1.1)\times10^{-6}$, $(4.6\pm1.8)\times10^{-6}$, $(6.1\pm1.5)\times10^{-6}$, and $(5.7\pm2.9)\times10^{-6}$, respectively. For accurate targeting of small plagioclase grains, we used a FIB (FEI Helios PFIB G4) to mark the measurement positions [9].

SIMS Methods: We used the WiscSIMS CAMECA IMS 1280 equipped with a high brightness radiofrequency (RF) plasma oxygen ion source for the Al-Mg isotope analyses [10-11]. The 3 μm diameter and 50 pA primary O_2^- ion beam was used for the analyses, which resulted in ~2×10^4 cps for ^{24}Mg intensity from the plagioclase standard with 0.1% MgO. We used a multicollector configuration with three electron multipliers (EM) for Mg isotopes and a Faraday cup for ^{27}Al. Acquisition time for each analysis was 40 min (10 s × 240 cycles), which resulted in counting errors (2SE) of the raw-measured δ^{25}Mg and mass fractionation corrected δ^{26}Mg* to be ~0.8‰ and ~1.6‰, respectively. The diameter of the final sputter crater was ~4 μm. Several natural plagioclase and synthetic anorthite glass standards were used for instrumental bias corrections.

EM gain adjustment: To keep the relative gain of the three EMs constant, we adjusted EM HV using CAMECA's standard algorithm. However, external reproducibility of δ^{26}Mg* was 2-3‰ for the plagioclase standard, probably due to inaccuracy of EM HV adjustment or unseen EM gain drifts [e.g. 12]. To improve reproducibility of Mg isotope analyses, we modified the EM pulse counting system according to [12] by adding a second discriminator in parallel as shown in Fig. 1. We monitored and calibrated EM gain drift during the analyses as a function of count ratios from two discriminators, with the second discriminator set to reject 50% of the total signal. By applying a gain correction based on the signal from the second discriminator, external reproducibility of δ^{26}Mg* in the plagioclase standard was improved to ~1.3‰.

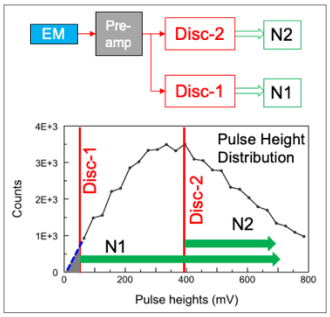

Fig. 1. Schematic diagram of modified EM pulse counting system, similar to [12]. Discriminator-2 is set to filter 50% of total counts. Changes in (N2/N1) reflect the shifts in pulse height distributions.

Results: For Y23, Y46, and Y58, 3 or 4 analyses of plagioclase were acquired in this work. For Y56, we only obtained one analyses. Four out of 12 analyses were stopped prior to the complete 240 cycles because the primary beam exposed Mg-rich inclusions. Some of the analyses show variability in ^{27}Al/^{24}Mg ratios much greater than those of the plagioclase standard, probably reflecting zoning in Mg contents in plagioclase or nm-scale inclusions enriched in Mg.

The results of Al-Mg isotope analyses are shown in Fig. 2. Our new data plot on the same isochron with the original dataset, but all show systematically higher ^{27}Al/^{24}Mg ratios and larger ^{26}Mg excesses. This is probably because the smaller primary beam and accurate targeting with FIB marks were helpful in analyzing clean plagioclase without overlapping Mg-rich inclusions and

adjacent mafic minerals. The isochron regression was made for each chondrule using both new and old datasets (Fig. 2). New regression lines are consistent with those from previous study [6], though precisions of regression lines are significantly improved by the factors of 2-4.

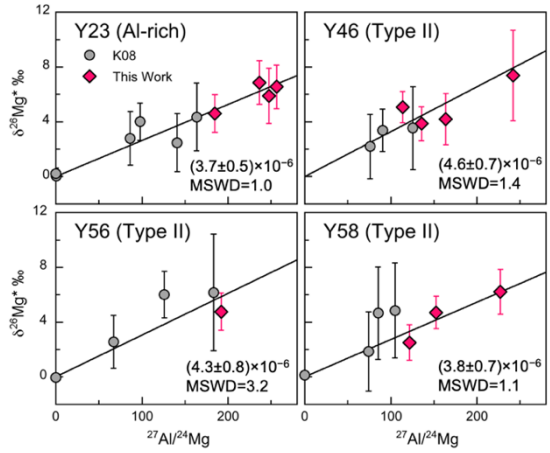

Fig. 2. Al-Mg isochron diagrams of chondrules in Y-81020. Circles and diamonds are data from [6] and this work, respectively. Inferred initial $(^{26}Al/^{27}Al)_0$ ratios and MSWD of regression lines are shown as inserts.

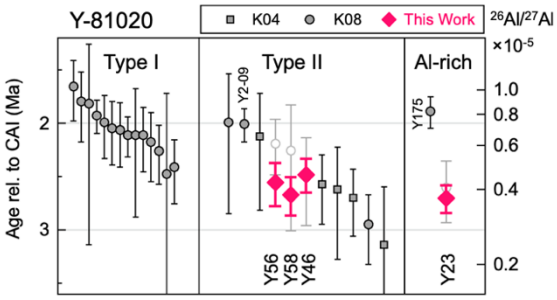

Fig. 3. Chondrule ^{26}Al ages in Y-81020 (CO3.05). Diamonds are those estimated from Fig. 2. Data from [5] and [6] are shown as squares and circles, respectively.

Discussions: The range of inferred initial $(^{26}Al/^{27}Al)_0$ ratios and relative ages among chondrules in Y-81020 are shown in Fig. 3. The revised datasets from the 3 type II chondrules are indistinguishable from each other and with good agreement to some type II chondrules analyzed by [5]. These 3 type II chondrules show systematically lower $(^{26}Al/^{27}Al)_0$ ~4×10^{-6} than those of most type I chondrules (~7×10^{-6} [6]), which was not obvious from old dataset [6]. They are clearly resolved from one of type II chondrules Y2-09, which is unusually abundant in Mg-rich olivine cores with $\Delta^{17}O$ values similar to those in type I chondrules [13]. Low $(^{26}Al/^{27}Al)_0$ of ARC Y23 is resolved from ARC Y175, which show distinct mineralogy from Y23 [6]. Thus, the ^{26}Al ages would be related to their chemical and isotope characters. The MSWDs of regression lines from three chondrules (except for Y56) are close to unity with large ranges of $^{27}Al/^{24}Mg$ ratios (100-250), suggesting that disturbance of the Al-Mg system from any parent body processes would be insignificant for these chondrules.

Our revised ^{26}Al age dataset of Y-81020 indicate that the meteorite contains chondrules that formed over a ~0.5 Ma time span. Chondrules accreted to CO chondrite parent body are from diverse origins that differ in time and space (and/or environments). Similarly, chondrules in Acfer 094 and CR chondrites contain chondrules with resolvable range of $(^{26}Al/^{27}Al)_0$ ratios [11, 14-19] that correlate with their Mg# and $\Delta^{17}O$ [17-19]. One possible mechanism for the observed diversity would be a transport in the disk [4, 19], which would deliver chondrules from inner disk regions to outer regions. Type I chondrules may have formed inside of the ice condensation front (snow line) in dry and reducing environments [e.g. 13, 20], then they may have been transported beyond the snow line where a majority of type II chondrules formed immediately before the CO3 parent body accretion.

Conclusions: New SIMS Al-Mg analytical methods (RF plasma ion source and improved multi-collection EM counting system) allow us to clearly resolve a small excess ^{26}Mg in chondrule plagioclase and improved the precision and accuracy of inferred $(^{26}Al/^{27}Al)_0$ estimates. Results suggest that type II chondrules formed later than type I chondrules in Y-81020 (CO3), by as much as 0.5 Ma. Higher precision Al-Mg chronology of chondrules would shed light on the locations and timing of chondrule formation and their potential transport mechanisms in the protoplanetary disk.

References: [1] Kita N. T. and Ushikubo T. (2012), *Meteoritics & Planet. Sci*., *47,* 1108–1119. [2] Cuzzi J. N. and Alexander C. M. O'D. (2006) *Nature, 441,* 483-485. [3] Alexander C. M. O'D. et al. (2008) *Science, 320,* 1617-1619. [4] Cuzzi J. N. et al. (2010) *Icarus, 208,* 518-538. [5] Kunihiro T. et al. (2004) *GCA, 68,* 2947-2957. [6] Kurahashi E. et al. (2008) *GCA, 72,* 3865-3882. [7] Larsen K. K. et al. (2011) *ApJ, 735,* L37(7pp). [8] Van Orman J. A. et al. (2014) *EPSL, 385,* 79-88. [9] Defouilloy C. et al. (2017) *EPSL, 465,* 145-154. [10] Kita N. T. et al. (2018) *LPS 49*, #2441. [11] Hertwig A. T. et al. (2018) *LPS 49,* #2061. [12] Hedberg P. M. L. et al. (2015) *J. Anal. At. Spectrom., 30,* 2516-2524. [13] Tenner T. J. et al. (2013) *GCA, 102,* 226-245. [14] Ushikubo T. (2013) *GCA*, *109*, 280–295. [15] Nagashima K. et al. *Geochem. J., 41,* 561-570. [16] Schrader D. et al. (2017) *GCA, 201,* 275-302. [17] Tenner T. J. (2015) *Meteoritics & Planet. Sci.*, *50,* #5325. [18] Tenner T. J. et al. (2019) *GCA, submitted*. [19] Hertwig A. T. et al. (2019) *GCA, revision*. [20] Tenner T. J. et al. (2015) *GCA, 148,* 228-250.